

PROBABILISTIC MODELLING USING EXPONENTIAL DISTRIBUTION FOR ENHANCED FATIGUE BEHAVIOUR UNDERSTANDING IN PLAIN CONCRETE

Haikhal Faez Hairuddin*, Mohamad Shazwan Ahmad Shah, Sarehati Umar, Ng Chiew Teng, Nurul 'Azizah Mukhlas

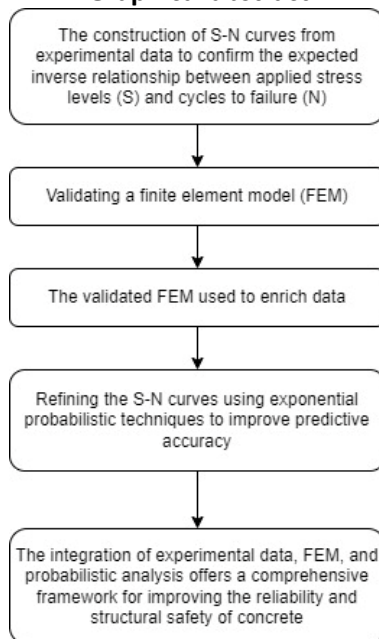
Department of Structure and Materials, Faculty of Civil Engineering, Universiti Teknologi Malaysia, 81310 UTM Johor Bahru, Malaysia

Article history

Received
12 September 2024
Received in revised form
22 December 2024
Accepted
23 December 2024
Published online
31 March 2025

*Corresponding author
haikhalfaez@graduate.utm.my

Graphical abstract



Abstract

This paper presents an in-depth study combining exponential probabilistic distribution and finite element analysis (FEA) to accurately predict the fatigue life of plain concrete subjected to cyclic loading. Existing fatigue life prediction models do not adequately address the variability and uncertainties inherent in concrete properties under cyclic loading. This is due to the complex nature of concrete and the time-consuming and challenging laboratory fatigue testing. Hence, the finite element method (FEM) was adopted as an alternative method in fatigue testing and the implementation of the probabilistic approach can account for these uncertainties and enhance the reliability of predictions. The research follows three primary stages: constructing S-N (stress-number of cycles) curves derived from experimental data across varying loading conditions, developing and validating a FEM in ABAQUS, and refining these S-N curves using exponential probabilistic techniques to improve predictive accuracy. Initial S-N curves from the experimental data confirmed the expected inverse relationship between applied stress levels and cycles to failure, consistent with classical fatigue behaviour in plain concrete. The FEM, validated using an optimal mesh size of 12 mm, achieved a high correlation with experimental data, evidenced by a minimal percentage error of just 0.80%, indicating high model fidelity. The validated FEM produced additional data points, complementing the experimental dataset. These were subsequently integrated into a probabilistic model using an exponential distribution, which enhanced the statistical representation of fatigue life predictions. This probabilistic model, driven by the exponential distribution, enabled the estimation of fatigue life across multiple confidence levels, with failure probabilities ranging from 99% to 20%, offering insights into the reliability of concrete structures under cyclic loads. The analysis further demonstrated that higher stress levels directly correlate with shortened fatigue lives and elevated rate parameters, indicating an accelerated rate of material degradation and highlighting the need for conservative stress design in concrete structures. This study underscores the essential role of integrating experimental data, FEM, and probabilistic analysis in advancing fatigue prediction methodologies by offering a comprehensive framework for improving reliability and structural safety, particularly under variable cyclic loading conditions.

Keywords: Fatigue life, finite element, water-cement ratio, probabilistic distribution, exponential distribution

© 2025 Penerbit UTM Press. All rights reserved

1.0 INTRODUCTION

Cyclic loading-induced fatigue has emerged as a critical issue in infrastructure systems like pavements, railway sleepers, bridge decks, and wind turbine towers, directly affecting the structural integrity and service life of these components (Ferreira et al., 2024). Over time, cyclic loading induces irreversible damage in concrete, often initiating as micro-cracks that propagate and coalesce into larger fractures, ultimately leading to structural failure. Due to its quasi-brittle behaviour, concrete is particularly vulnerable to fatigue loading, which can cause more severe and progressive damage compared to static loads, even when the applied stress levels are lower (Renju & Keerthy, 2020; Zhang & Wang, 2021). Therefore, a comprehensive understanding of concrete fatigue behaviour is critical for developing durable, long-lasting structures, particularly in high-cycle applications where repeated loading can severely shorten service life (Xu et al., 2021).

Conventional fatigue life evaluation methods frequently fail to account for the inherent variability in material properties, such as microstructural differences, even within specimens from the same production batch. To address this issue, it is necessary to employ larger sample sizes and integrate robust statistical modelling approaches, rather than relying on limited specimen counts or simplistic average-based analyses (Ferreira et al., 2023). Several challenges have been identified in this research, particularly with deterministic models such as S-N curves, which, while insightful, struggle to capture the full complexity of concrete's fatigue behaviour under varying stress conditions (Renju & Keerthy, 2020). Additionally, conventional experimental testing presents challenges in terms of extended testing durations, precision in data collection, and the need for controlled test environments, prompting the integration of advanced techniques like finite element analysis (FEA) (Ghandriz et al., 2020).

Moreover, the inherent complexity and scarcity of comprehensive fatigue data necessitate the adoption of probabilistic approaches which could effectively account for material and loading uncertainties, thus enhancing the reliability and robustness of fatigue life predictions (Renju & Keerthy, 2020). Since fatigue data was skewed, skewed distributions such as Weibull, lognormal, exponential, and Gamma distributions can be used to model fatigue data. However, in this study, the exponential distribution was utilised as it is more flexible for analysing skewed data since it was a one-parameter distribution unlike the other distributions mentioned (Raza et al., 2024).

The primary objective of this study is to construct detailed S-N curves for plain concrete, subjected to multiple loading scenarios—including varying stress levels and water-cement ratios—using high-fidelity experimental data. The second objective is to simulate the experimental results using ABAQUS, developing a high-accuracy finite element model capable of predicting fatigue behaviour under a range of cyclic loading conditions. The final objective is to create an integrated numerical model combining deterministic methods, such as FEM, with probabilistic approaches—namely, exponential distribution modelling—to more accurately predict the fatigue life of plain concrete, accounting for material variability and loading uncertainties.

In this study, S-N curves are constructed for plain concrete, incorporating key variables such as applied stress levels and water-cement ratios to accurately capture the material's fatigue

performance under cyclic loading. Experimental data from prior studies on plain concrete fatigue will be utilised to validate the finite element model developed in ABAQUS, ensuring the model's accuracy across a range of material behaviours. Probabilistic methods, including exponential distribution, are subsequently applied to augment the dataset, explicitly addressing uncertainties in material properties, cyclic loading conditions, and structural variability, thereby improving the predictive accuracy of fatigue life estimates. This study aims to provide actionable insights for optimising the design and fatigue assessment of concrete structures, ultimately contributing to more reliable and durable construction practices through advanced fatigue modelling techniques.

2.0 METHODOLOGY

This section outlines a detailed methodology developed to achieve the research objectives. The study is structured into three major stages: constructing S-N curves using experimental data, developing and validating a finite element model (FEM) in ABAQUS, and applying probabilistic modelling techniques to refine the S-N curves. Each step is discussed comprehensively below.

2.1 Construction of S-N Curve

The construction of S-N curves for plain concrete is based on experimental data from concrete beams subjected to varying stress levels and cyclic loading. The concrete beams used in this study had a water-cement ratio of 0.4, in accordance with the RILEM Recommendations: TC 89-FMT. The final beam dimensions were 1065 mm in length, 110 mm in width, and 100 mm in depth, providing sufficient representation of a typical concrete member used in civil infrastructure. The ultimate flexural strength of the beams under static loading was determined to be 6.53 MPa, serving as a baseline for subsequent fatigue tests. Fatigue testing was conducted under the three-point bending test configuration as shown in Figure 1, following the American Concrete Institute (ACI) 215R-74 standards, which dictate procedures for evaluating the fatigue strength of plain concrete.



Figure 1 Three-point bending test configuration for fatigue testing.

A cyclic loading frequency of 30 Hz was employed for all specimens, with maximum flexural stress levels set at 74.6%, 70%, 68.9%, 61.2%, 52.5%, and 35% of the ultimate flexural strength, corresponding to 4.87 MPa, 4.568 MPa, 4.497 MPa, 3.997 MPa, 3.426 MPa, and 2.286 MPa, respectively. These stress levels were selected to cover a broad range of fatigue performance and capture the transition between high and low fatigue lives.

For each stress level, the number of cycles to failure was recorded. This data was subsequently plotted to generate the S-N curves, illustrating the relationship between applied stress and fatigue life (number of cycles to failure). These curves served as the foundational dataset for model validation and probabilistic analysis in the later stages of the research.

2.2 Finite Element Analysis (FEA)

Finite element analysis (FEA) was conducted to simulate the fatigue performance of the plain concrete beams and to validate the experimental results. The FEA model was developed using the ABAQUS software, following the specific setup and configuration detailed below.

2.2.1 Part Module

In the ABAQUS part module, as shown in Figure 2, the beam geometry was defined as a 3D solid with dimensions of 1065 mm in length, 110 mm in width, and 100 mm in depth, consistent with the experimental specimens. The beam was modelled as deformable, and the shape was extruded to match the dimensions used in experimental testing. Support conditions were replicated using two fixed support lines located 132.5 mm from the beam edges to simulate a three-point bending test with an effective span of 800 mm. An additional line was drawn at the midpoint of the beam's top surface to apply the cyclic loading in the simulation.

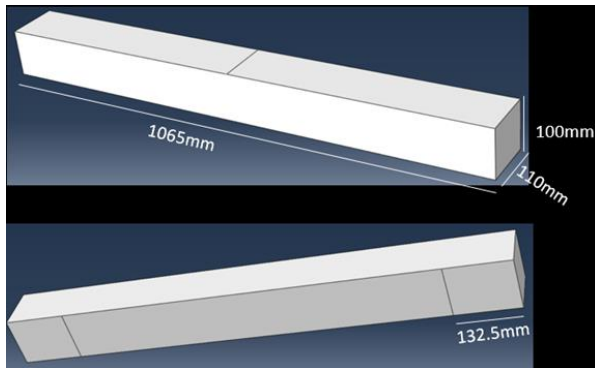


Figure 2 Beam specimen created in part module

2.2.2 Properties Module

Since the material used was concrete, the nonlinear concrete model was adopted. The material properties of the plain concrete were defined using both elastic and plastic parameters. The density of the concrete was set to $2.4 \times 10^{-5} \text{ kg/mm}^3$, with Young's modulus and Poisson's ratio defined as 14,176 MPa and 0.2, respectively. For the plastic properties, the yield stress was determined to be 14.438 MPa, and the plastic strain was set to zero. The damage evolution was modelled using the maximum

principal stress, with a maximum principal stress value of 6.53 MPa and a displacement at failure of 0.45 mm. These material properties were selected based on the experimentally determined static flexural strength of the concrete beams.

2.2.3 Assembly and Step Modules

The beam model was then assembled, with all boundary conditions set to simulate a three-point bending test. The loading step was defined as "Static, General" under the ABAQUS step module, with a time period of 50 seconds to mirror the real-world experimental loading conditions. The maximum number of increments was set to 10,000, and the initial, minimum, and maximum increment sizes were defined as 0.1, 0.01, and 1, respectively. These increment settings ensured that even small changes in stress and strain during the loading cycles were captured accurately.

2.2.4 Load and Interaction Modules

In the load module, a concentrated force was applied at the reference point located at the centerline of the beam's top surface as shown in Figure 3. The force magnitude was calculated based on the maximum flexural stress values from the experimental data using the following equation:

$$P = \frac{2 \cdot B \cdot H^2 \cdot \sigma_{bend,max}}{3 \cdot S \cdot \sigma_{bend,max} \cdot 0.425}$$

Where:

- P = applied load,
- B = beam width,
- H = beam height,
- $\sigma_{bend,max}$ = maximum flexural stress,
- S = effective span.

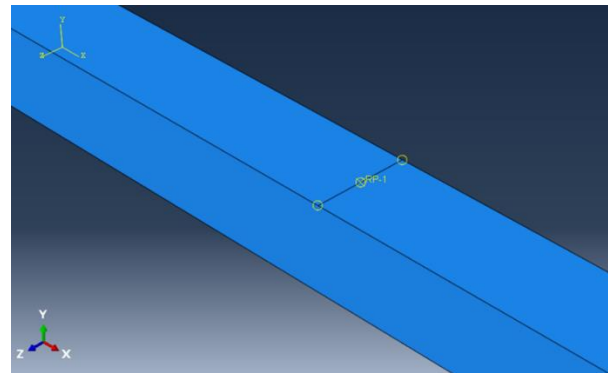


Figure 3 Reference point created at the line drawn marked as RP-1

The boundary conditions constrained the movement of the beam in all directions at the support points, accurately replicating the experimental setup. To simulate cyclic loading, a periodic amplitude function was applied using a constant amplitude sine wave at a frequency of 30 Hz.

2.2.5 Mesh Module

Meshing is a critical step in FEA that influences the accuracy of the simulation results. A mesh convergence study was

conducted to determine the optimal mesh size for the beam model. Mesh sizes of 8 mm, 10 mm, 12 mm, 14 mm, 15 mm, 20 mm, 25 mm, and 30 mm were tested. The 12 mm mesh size, which generated 6,408 elements, was found to provide the closest match to the experimental data, with a minimal percentage difference of just 0.80%. This mesh size was therefore used for all subsequent simulations to ensure both accuracy and computational efficiency.

2.3 Data Validation

Data from the finite element model was validated against experimental results by calculating the percentage difference between the two datasets. For each stress level, the number of cycles to failure predicted by the FEM was compared to the experimentally observed values. The results of the comparison, summarized in Table 2, showed that all percentage differences were below 10%, further verifying the accuracy and reliability of the FEM in simulating concrete fatigue under cyclic loading.

2.4 Application of Probabilistic Distribution

To enhance the predictive capability of the fatigue life model, a probabilistic approach using exponential distribution was applied. A total of 14 data points, including both experimental data and additional FEM-generated points, were used to develop the probabilistic model. The first step involved transforming the S-N data (stress and cycles to failure) into their natural logarithmic form to linearise the relationship between stress and fatigue life.

Regression analysis was then performed on the transformed data to determine the slope (b) and intercept ($\ln(a)$) of the regression line, which are essential parameters for modelling fatigue life. These values were calculated using the following equations:

$$S = aN^b$$

Regression analysis provided the slope (b) and intercept ($\ln(a)$) for the S-N equation by using equations as follows:

$$b = \frac{n \sum(\ln(N) \cdot \ln(S)) - \sum(\ln(N)) \cdot \sum(\ln(S))}{n \sum(\ln(N)^2) - (\sum(\ln(N)))^2}$$

$$\ln(a) = \frac{\sum(\ln(S)) - b \sum(\ln(N))}{n}$$

Once the regression parameters were obtained, the mean number of cycles to failure at each stress level was calculated using the following equation:

$$N\mu = \left(\frac{S}{a}\right)^{\frac{1}{b}}$$

The rate parameter (λ) was then determined as:

$$\lambda = \frac{1}{N\mu}$$

The exponential distribution was used to estimate the number of cycles to failure at different probability levels, ranging from 99% to 20%, using the following equation:

$$F(x; \lambda) = 1 - e^{-\lambda x}$$

This probabilistic model provides a more nuanced understanding of the variability in fatigue life under different stress levels and helps improve the reliability of fatigue life predictions (Sohel et al., 2022).

3.0 RESULTS AND DISCUSSION

The results of this study are based on the integration of experimental data, finite element analysis (FEA), and probabilistic modelling to develop a comprehensive S-N curve for plain concrete under cyclic loading. The discussion focuses on the accuracy of the finite element model, the enhancement of the S-N curve through probabilistic modelling, and the implications of the findings for fatigue life prediction in plain concrete.

3.1 S-N Curve Development

The experimental data collected from fatigue testing of plain concrete beams under varying stress levels are presented in an S-N curve manner as shown in Figure 4. The stress levels started from 2.286, 3.426, 3.997, 4.497, 4.568, and 4.87 MPa, with their corresponding number of cycles to failure.

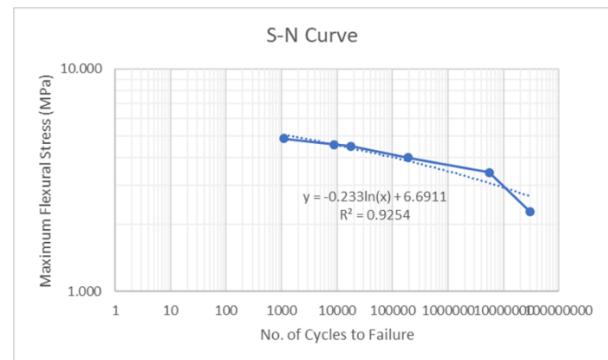


Figure 4 S-N curve from experimental data

Based on Figure 4, as the stress levels increase, the fatigue life decreases which agrees with the general inverse relationship between applied stress and fatigue life (Wang, Li, et al., 2024). The x-axis represents the number of cycles to failure (N), while the y-axis corresponds to the applied stress (S), both plotted on a logarithmic scale. The trendline added to the S-N curve follows a logarithmic equation with a high correlation coefficient ($R^2 = 0.9254$), indicating a strong fit between the experimental data and the logarithmic model. The logarithmic nature of the curve is consistent with classical fatigue theory, where the number of cycles to failure decreases as the applied stress increases (Wang, Li, et al., 2024). This behaviour highlights the importance of maintaining low-stress levels in concrete structures subjected to cyclic loading to prevent premature failure.

3.2 Mesh Convergence Study

The accuracy of the FEM depends heavily on the mesh size. A mesh convergence study was conducted using eight different

mesh sizes, ranging from 8 mm to 30 mm. The relationship in mesh convergence often relates the stress to the number of elements. When the mesh is applied to the specimen, the specimen is divided into smaller partitions called the element. The number of elements increases as the mesh size decreases. Technically, the optimum mesh size was determined at the lowest difference between the maximum principal stress from the FEA simulation produced by the respective mesh size and the maximum flexural stress from experimental data which in this case was 4.87 MPa. By varying the different mesh sizes while maintaining the other parameter values in other modules, the results can be obtained and recorded in Table 1. The percentage difference can be determined using the equation below.

$$\text{Difference}(\%) = \frac{\text{Max Principal Stress} - 4.87}{4.87} \times 100\%$$

Table 1 Comparison between experiment data and finite element data for different mesh size

Mesh Size (mm)	No. of Element	Max. Principal Stress (MPa)	Percentage Difference (%)
8	24388	5.305	8.93
10	11660	5.096	4.64
12	6408	4.909	0.80
14	4256	4.776	1.93
15	3528	4.771	2.03
20	1620	4.458	8.46
25	672	4.254	12.65
30	432	3.835	21.25

Based on Table 1, the maximum error calculated was 21.25% for a mesh size of 30 mm while the minimum error was 0.80% for a mesh size of 12 mm. A mesh size of 30 mm contains only 432 elements, which means that each element is too large to capture variations in the specimen's properties accurately. For example, when a load is applied to a specific location on the beam, if the coverage area of a single element exceeds the affected area, the impact will be averaged over the areas that are not influenced by the loading. As a result, the loading effect becomes insignificant for the specimen. In contrast, with a mesh size of 8 mm, the number of elements increased to 24388, indicating that each element is significantly smaller relative to the specimen size. This allows the affected area to become more significant for the specimen. Consequently, the impact of the loading surpasses the optimal result resulting in a large difference. Hence, the mesh size of 12 mm was determined as the optimum mesh size since the size produced the lowest percentage difference.

3.3 Finite Element Model Validation

Once the optimal mesh size was established, the finite element model was validated against the experimental results. Table 2 presents a comparison of the maximum principal stresses and the corresponding percentage differences between the experimental data and the FEM simulation results for each stress level. The FEM results were within 10% of the experimental values for all stress levels, with the smallest difference being 0.70% and the largest difference being 6.58%. This high level of

agreement between the FEM and experimental data confirms that the finite element model is capable of accurately simulating the fatigue behaviour of plain concrete beams under cyclic loading.

Table 2 Percentage difference between experimental and finite element data

Experiment Data (MPa)	Finite Element Data (MPa)	Percentage Difference (%)
4.870	4.909	0.80
4.568	4.457	2.43
4.497	4.202	6.56
3.997	4.260	6.58
3.426	4.254	5.02
2.286	2.302	0.70

The validated FEM model was then used to generate additional data points for stress levels not covered in the experimental testing. These additional data points were incorporated into the S-N curve to enhance its robustness and to fill gaps in the experimental dataset. By enriching the S-N curve with FEM-generated data, a more comprehensive representation of fatigue life across a wider range of stress levels was obtained, as shown in Figure 5.

3.4 Data Enrichment and Probabilistic Modelling Using Exponential Distribution

By varying the stress applied, the corresponding fatigue life can be obtained through the simulation of the validated FEM. The data was enriched with an additional eight data points from the existing six experimental data points resulting in a total of 14 data points. The combination of FEM data and experimental data was tabulated in Table 3. To visualise the result graphically, the data was plotted in an S-N curve manner as shown in Figure 5. It is remarked that the data represent the mean value since the average data was calculated based on laboratory fatigue testing. Thus, the data must be interpreted with the consideration for variability and uncertainty in real-world applications.

Table 3 Combined data from experimental data and finite element analysis

Stress (S)	No. of Cycle to Failure (N _f)
2.286	30000000
2.368	26567010
2.589	20191920
3.140	11818650
3.426	5533560
3.598	3999000
3.606	2764929
3.997	191524
4.056	165420
4.339	17465
4.497	15845
4.568	8855
4.685	4985
4.870	1115

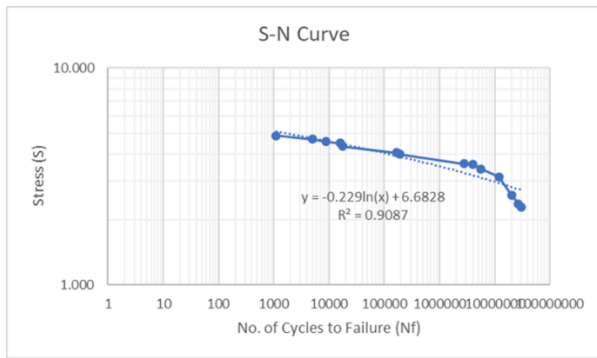


Figure 5 S-N curve corresponds to Table 3

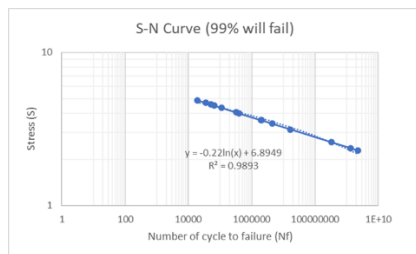
Hence, to address the issues, the exponential distribution was employed on the combined data in Table 3, to enhance reliability in engineering designs. By employing the exponential distribution, the corresponding mean number of cycles to failure (N_{μ}) was calculated for each stress level. The rate parameter (λ) for the exponential distribution was then determined, as shown in Table 4. The rate parameter reflects the degradation rate of the material under cyclic loading, with higher stress levels resulting in higher rate parameters and shorter fatigue lives.

Table 4 Mean cycle to failure and rate parameter

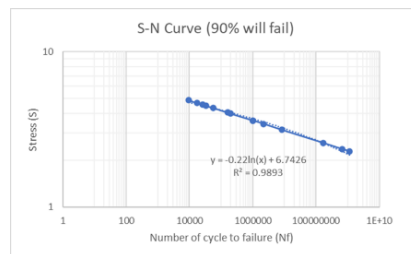
No	Stress (S)	Mean cycle to failure (N_{μ})	Rate Parameter (λ)
1	2.286	494159188.8	2.02364E-09
2	2.368	285693584.6	3.50025E-09
3	2.589	71967158.02	1.38952E-08
4	3.140	3650086.811	2.73966E-07
5	3.426	949139.5276	1.05359E-06
6	3.598	445255.8793	2.2459E-06
7	3.606	430234.6027	2.32431E-06
8	3.997	87674.98743	1.14058E-05
9	4.056	69910.59725	1.4304E-05
10	4.339	24656.46789	4.05573E-05
11	4.497	14197.48645	7.0435E-05
12	4.568	11137.57386	8.97862E-05
13	4.685	7534.852877	0.000132717
14	4.870	4137.808892	0.000241674

To enhance the comprehensive understanding of the variability in fatigue life and enable the prediction of failure probabilities at various confidence levels, the exponential distribution was used to estimate the number of cycles to failure at different probabilities, ranging from 99% to 20%. The

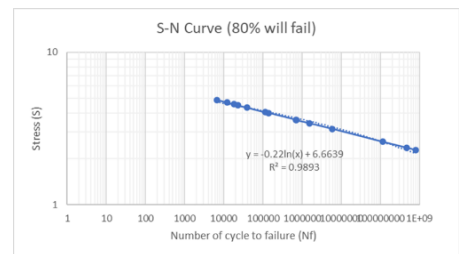
probability levels at 99%, 90%, 80%, 50% and 20% were applied to the data to find the number of cycles to failure corresponding to the probability level. The results for each probability level were visualised graphically in an S-N curve manner as shown in Figure 6.



(a)



(b)



(c)

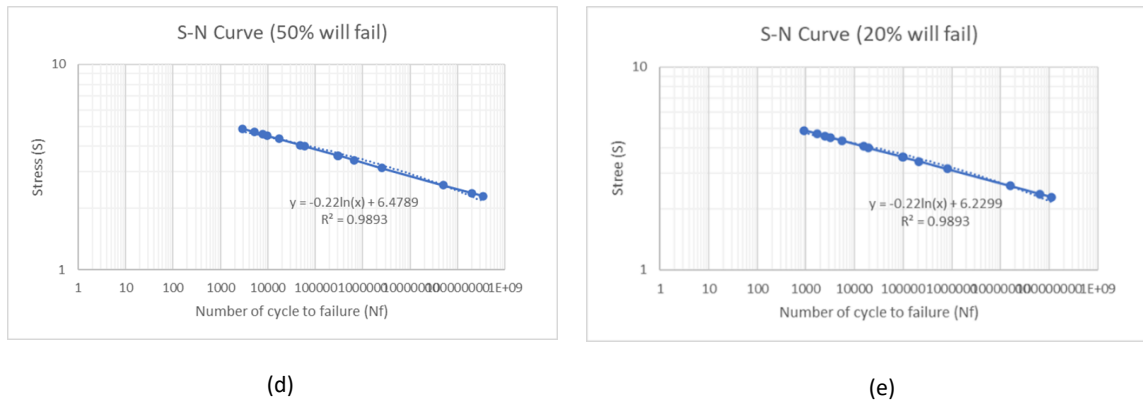


Figure 6 S-N curves for the plain concrete beam to fail at (a) 99%, (b) 90%, (c) 80%, (d) 50%, and (e) 20% probability, respectively.

Based on Figure 6, it can be seen that as the probability decreases, the estimated number of cycles to failure also decreases, reflecting the higher likelihood of failure at lower cycle counts. Furthermore, these ranges can give a better insight into the fatigue behaviour which helps in having a better engineering design that better reflects the real-world application.

This probabilistic model significantly enhances the reliability of fatigue life predictions by accounting for uncertainties that are not captured by deterministic methods. For example, at a 99% probability, the beam is predicted to fail after a relatively high number of cycles, indicating a high level of confidence in the material's fatigue performance. Conversely, at a 20% probability, the beam is expected to fail much earlier, reflecting a more conservative estimate of fatigue life. This approach allows engineers to choose appropriate design factors based on the required safety and reliability levels for specific concrete structures.

3.5 Discussion and Implications

The results of this study provide valuable insights into the fatigue behaviour of plain concrete under cyclic loading. The integration of experimental data, finite element analysis, and probabilistic modelling offers a robust framework for improving the accuracy of fatigue life predictions. The validated FEM model, with a mesh size of 12 mm, demonstrated a high level of accuracy, with all percentage differences between the FEM and experimental data falling below 10%. This confirms the reliability of the FEM in simulating the laboratory fatigue testing.

The probabilistic modelling approach using exponential distribution further enriched the S-N curve, allowing for more nuanced predictions of fatigue life at different probability levels. This model accounts for the inherent variability in concrete materials and loading conditions, providing a more realistic representation of fatigue performance. The findings suggest that higher stress levels lead to faster material degradation and shorter fatigue lives, emphasizing the importance of maintaining conservative stress levels in the design of concrete structures subjected to cyclic loading.

From a practical perspective, the enhanced S-N curve and probabilistic model developed in this study can be used to improve the design and maintenance strategies for concrete structures, such as pavements, bridge decks, and wind turbine towers. By providing more accurate predictions of fatigue life,

this approach helps engineers optimise the use of materials and resources, reducing the risk of premature failure and extending the service life of critical infrastructure components.

4.0 CONCLUSION

This study provides a detailed investigation into the fatigue behaviour of plain concrete using a combination of experimental data, finite element analysis (FEA), and probabilistic modelling. The integration of these three methodologies offers a more accurate and reliable prediction framework for fatigue life in concrete structures subjected to cyclic loading.

The experimental phase established S-N curves that confirmed the inverse relationship between applied stress levels and the number of cycles to failure, consistent with classical fatigue theory. The finite element model (FEM), developed and validated using experimental data, demonstrated excellent accuracy, with a percentage difference of less than 10% for all stress levels. The optimal mesh size of 12 mm provided the best balance between computational efficiency and result accuracy. This validated FEM model was used to generate additional data points, enriching the experimental dataset and enhancing the robustness of the S-N curves.

The application of exponential probabilistic distribution modelling allowed for the incorporation of material variability and uncertainties into fatigue life predictions. By estimating the number of cycles to failure at different probabilities (99%, 90%, 80%, 50%, and 20%), the model provided a more comprehensive understanding of fatigue performance. This probabilistic approach enhances the accuracy and reliability of predictions, offering valuable insights for optimising the design and maintenance of concrete structures subjected to cyclic loading.

The findings of this research have significant implications for the civil engineering field. The integration of experimental data, FEM, and probabilistic models can be used to improve the design of durable concrete structures, such as pavements, bridge decks, and wind turbine towers, by offering more accurate fatigue life predictions. The study emphasizes the importance of using advanced modelling techniques to account for material variability and loading uncertainties, ensuring the safety and longevity of critical infrastructure.

Future work should explore the extension of this methodology to other concrete types, such as reinforced or fibre-reinforced concrete, and examine the impact of

environmental factors on fatigue performance. Incorporating reinforcement and composite materials into the fatigue modelling process can provide a broader understanding of fatigue behaviour in more complex structural systems.

Acknowledgements

The authors would like to express their sincere gratitude to Universiti Teknologi Malaysia (UTM) for providing the necessary resources and facilities that made this research possible. The authors also gratefully acknowledge the financial support from the Malaysia Ministry of Higher Education (MoHE) under the research grant PY/2023/02180 (R.J130000.7822.5F661). This support played a crucial role in the successful completion of this research.

Conflicts of Interest

The author(s) declare(s) that there is no conflict of interest regarding the publication of this paper

References

- [1] Abambres, M., & Lantsoght, E. O. L. 2019. ANN-based fatigue strength of concrete under compression. *Materials*, 12(22). <https://doi.org/10.3390/ma12223787>
- [2] Alrayes, O., Könke, C., Ooi, E. T., & Hamdia, K. M. 2023. Modeling Cyclic Crack Propagation in Concrete Using the Scaled Boundary Finite Element Method Coupled with the Cumulative Damage-Plasticity Constitutive Law. *Materials*, 16(2). <https://doi.org/10.3390/ma16020863>
- [3] Al-Saoudi, A., Al-Mahaidi, R., Kalfat, R., & Cervenka, J. 2019. Finite element investigation of the fatigue performance of FRP laminates bonded to concrete. *Composite Structures*, 208: 322–337. <https://doi.org/10.1016/j.compstruct.2018.10.001>
- [4] Baktheer, A. 2019. Microplane damage plastic model for plain concrete subjected to compressive fatigue loading. 10th *International Conference on Fracture Mechanics of Concrete and Concrete Structures*. 1-12. <https://doi.org/10.21012/fc10.233196>
- [5] Baktheer, A., & Becks, H. 2021. Fracture mechanics based interpretation of the load sequence effect in the flexural fatigue behavior of concrete using digital image correlation. *Construction and Building Materials*, 307. <https://doi.org/10.1016/j.conbuildmat.2021.124817>
- [6] Baktheer, A., & Chudoba, R. 2021. Experimental and theoretical evidence for the load sequence effect in the compressive fatigue behavior of concrete. *Materials and Structures/Materiaux et Constructions*, 54(2). <https://doi.org/10.1617/s11527-021-01667-0>
- [7] Blasón, S., Poveda, E., Ruiz, G., Cifuentes, H., & Fernández Canteli, A. 2019. Twofold normalization of the cyclic creep curve of plain and steel-fiber reinforced concrete and its application to predict fatigue failure. *International Journal of Fatigue*, 120: 215–227. <https://doi.org/10.1016/j.ijfatigue.2018.11.021>
- [8] Chen, H., Sun, Z., Zhong, Z., & Huang, Y. 2022. Fatigue Factor Assessment and Life Prediction of Concrete Based on Bayesian Regularized BP Neural Network. *Materials*, 15(13). <https://doi.org/10.3390/ma15134491>
- [9] Deutscher, M., Tran, N. L., & Scheerer, S. 2019. Experimental investigations on the temperature increase of ultra-high performance concrete under fatigue loading. *Applied Sciences (Switzerland)*, 9(19). <https://doi.org/10.3390/app9194087>
- [10] Fan, Z., & Sun, Y. 2019. Detecting and evaluation of fatigue damage in concrete with industrial computed tomography technology. *Construction and Building Materials*, 223: 794–805. <https://doi.org/10.1016/j.conbuildmat.2019.07.016>
- [11] Ferreira, E. C., Sotoudeh, P., Fiorillo, G., & Svecova, D. 2023. The probabilistic fatigue life of plain concrete under low-frequency stress reversal loading. In *Life-Cycle of Structures and Infrastructure Systems* 3492–3499. CRC Press. <https://doi.org/10.1201/9781003323020-427>
- [12] Ferreira, E., Sotoudeh, P., & Svecova, D. 2024. Fatigue life of plain concrete subjected to low frequency uniaxial stress reversal loading. *Construction and Building Materials*, 411. <https://doi.org/10.1016/j.conbuildmat.2023.134247>
- [13] Gao, D., Gu, Z., Zhu, H., & Huang, Y. 2020. Fatigue behavior assessment for steel fiber reinforced concrete beams through experiment and Fatigue Prediction Model. *Structures*, 27: 1105–1117. <https://doi.org/10.1016/j.istruc.2020.07.028>
- [14] Ghandriz, R., Hart, K., & Li, J. 2020. Extended finite element method (XFEM) modeling of fracture in additively manufactured polymers. *Additive Manufacturing*, 31. <https://doi.org/10.1016/j.addma.2019.100945>
- [15] Ge, B., & Kim, S. 2021. Probabilistic service life prediction updating with inspection information for RC structures subjected to coupled corrosion and fatigue. *Engineering Structures*, 238. <https://doi.org/10.1016/j.engstruct.2021.112260>
- [16] Guo, X., Wang, Y., Huang, P., & Chen, Z. 2019. Finite element modeling for fatigue life prediction of RC beam strengthened with prestressed CFRP based on failure modes. *Composite Structures*, 226. <https://doi.org/10.1016/j.compstruct.2019.111289>
- [17] Huang, J., Qiu, S., & Rodrigue, D. (2022). Parameters estimation and fatigue life prediction of sisal fibre reinforced foam concrete. *Journal of Materials Research and Technology*, 20: 381–396. <https://doi.org/10.1016/j.jmrt.2022.07.096>
- [18] Kachkouch, F. Z., Noberto, C. C., de Albuquerque Lima Babadopulos, L. F., Melo, A. R. S., Machado, A. M. L., Sebaibi, N., Boukhelf, F., & El Mendili, Y. 2022. Fatigue behavior of concrete: A literature review on the main relevant parameters. In *Construction and Building Materials* 338. Elsevier Ltd. <https://doi.org/10.1016/j.conbuildmat.2022.127510>
- [19] Kasu, S. R., Deb, S., Mitra, N., Muppireddy, A. R., & Kusam, S. R. 2019. Influence of aggregate size on flexural fatigue response of concrete. *Construction and Building Materials*, 229. <https://doi.org/10.1016/j.conbuildmat.2019.116922>
- [20] Keerthana, K., & Kishen, J. M. C. (2020). Micromechanics of fracture and failure in concrete under monotonic and fatigue loadings. *Mechanics of Materials*, 148. <https://doi.org/10.1016/j.mechmat.2020.103490>
- [21] Lee, J., Jeon, C. H., Shim, C. S., & Lee, Y. J. 2023. Bayesian inference of pit corrosion in prestressing strands using Markov Chain Monte Carlo method. *Probabilistic Engineering Mechanics*, 74. <https://doi.org/10.1016/j.proengmech.2023.103512>
- [22] Liu, W. K., Li, S., & Park, H. S. 2022. Eighty Years of the Finite Element Method: Birth, Evolution, and Future. In *Archives of Computational Methods in Engineering*. 29(6): 4431–4453. Springer Science and Business Media B.V. <https://doi.org/10.1007/s11831-022-09740-9>
- [23] Rastayesh, S., Mankar, A., Sørensen, J. D., & Bahrebar, S. 2020. Development of stochastic fatigue model of reinforcement for reliability of concrete structures. *Applied Sciences (Switzerland)*, 10(2). <https://doi.org/10.3390/app10020604>
- [24] Raza, A., Ali, S., Shah, I., Al-Rezami, A. Y., & Almazah, M. M. A. 2024. A comparative analysis of mean charts assuming Weibull and generalized exponential distributions. *Heliyon*, 10(21): e40001. <https://doi.org/10.1016/j.heliyon.2024.e40001>

- [25] Renju, D. R., & Keerthy, M. S. 2020. A Review on Fatigue Life Prediction of Plain Concrete. *IOP Conference Series: Materials Science and Engineering*, 936(1). <https://doi.org/10.1088/1757-899X/936/1/012026>
- [26] Riyar, R. L., Mansi, & Bhowmik, S. 2023. Fatigue behaviour of plain and reinforced concrete: A systematic review. *Theoretical and Applied Fracture Mechanics*, 125. <https://doi.org/10.1016/j.tafmec.2023.103867>
- [27] Sainz-Aja, J., Thomas, C., Carrascal, I., Polanco, J. A., & de Brito, J. 2020. Fast fatigue method for self-compacting recycled aggregate concrete characterization. *Journal of Cleaner Production*, 277. <https://doi.org/10.1016/j.jclepro.2020.123263>
- [28] Sainz-Aja, J., Thomas, C., Polanco, J. A., & Carrascal, I. 2020. High-frequency fatigue testing of recycled aggregate concrete. *Applied Sciences (Switzerland)*, 10(1). <https://doi.org/10.3390/app10010010>
- [29] Sohel, K. M. A., Al-Hinai, M. H. S., Alnuaimi, A., Al-Shahri, M., & El-Gamal, S. 2022. Prediction of flexural fatigue life and failure probability of normal weight concrete. *Materiales de Construccion*, 72(347). <https://doi.org/10.3989/MC.2022.03521>
- [30] Sun, B., & Xu, Z. 2021. An efficient numerical method for meso-scopic fatigue damage analysis of heterogeneous concrete. *Construction and Building Materials*, 278. <https://doi.org/10.1016/j.conbuildmat.2021.122395>
- [31] Sun, J., Ding, Z., & Huang, Q. 2019. Corrosion fatigue life prediction for steel bar in concrete based on fatigue crack propagation and equivalent initial flaw size. *Construction and Building Materials*, 195, 208–217. <https://doi.org/10.1016/j.conbuildmat.2018.11.056>
- [32] Velarde, J., Kramhøf, C., Mankar, A., & Sørensen, J. 2019. Uncertainty modeling and fatigue reliability assessment of offshore wind turbine concrete structures. *International Journal of Offshore and Polar Engineering*, 29(2): 165–174. <https://doi.org/10.17736/ijope.2019.il54>
- [33] Wang, Y. L., Guo, X. Y., Huang, P. Y., Huang, K. N., Yang, Y., & Chen, Z. B. 2020. Finite element investigation of fatigue performance of CFRP-strengthened beams in hygrothermal environments. *Composite Structures*, 234. <https://doi.org/10.1016/j.compstruct.2019.111676>
- [34] Wang, Y., Li, Y., Lu, L., Wang, F., Wang, L., Liu, Z., & Jiang, J. 2024. Numerical prediction for life of damaged concrete under the action of fatigue loads. *Engineering Failure Analysis*, 162, 108368. <https://doi.org/10.1016/j.engfailanal.2024.108368>
- [35] Wu, J., Zhang, B., Xu, J., Jin, L., & Diao, B. 2023. Probabilistic fatigue life prediction for RC beams under chloride environment considering the statistical uncertainty by Bayesian updating. *International Journal of Fatigue*, 173. <https://doi.org/10.1016/j.ijfatigue.2023.107680>
- [36] Xu, L., Ma, M., Li, L., Xiong, Y., & Liu, W. 2021. Continuum-based approach for modelling the flexural behaviour of plain concrete beam under high-cycle fatigue loads. *Engineering Structures*, 241. <https://doi.org/10.1016/j.engstruct.2021.112442>
- [37] Yadav, I. N., & Thapa, K. B. 2020. Fatigue damage model of concrete materials. *Theoretical and Applied Fracture Mechanics*, 108. <https://doi.org/10.1016/j.tafmec.2020.102578>
- [38] Zhang, Q., & Wang, L. 2021. Investigation of stress level on fatigue performance of plain concrete based on energy dissipation method. *Construction and Building Materials*, 269. <https://doi.org/10.1016/j.conbuildmat.2020.121287>